Development 134, 3999-4009 (2007) doi:10.1242/dev.002741

Co-regulation by Notch and Fos is required for cell fate specification of intermediate precursors during *C. elegans* uterine development

Kavita S. Oommen[1] and Anna P. Newman[1,2,3,*]

The Notch pathway is the key signal for many cell fate decisions in the nematode *Caenorhabditis elegans* including the uterine π cell fate, crucial for a proper uterine-vulval connection and egg laying. Expression of the *egl-13* SOX domain transcription factor is specifically upregulated upon induction of the π lineage and not in response to other LIN-12/Notch-mediated decisions. We determined that dual regulation by LIN-12 and FOS-1 is required for *egl-13* expression at specification and for complete rescue of *egl-13* mutants. We found that *fos-1* mutants exhibit uterine defects and fail to express π markers. We show that FOS-1 is expressed at π cell specification and can bind in vitro to *egl-13* upstream regulatory sequence (URS) as a heterodimer with *C. elegans* Jun.

KEY WORDS: LIN-12, Notch, LAG-1, CSL, FOS-1, Fos, Jun, Specification, Transcription

INTRODUCTION

The Notch pathway specifies numerous cell fates during development. How can diverse tissues be generated under the control of a single reiteratively utilized pathway? Understanding mechanisms that directly influence target gene expression may provide insights into how this critical pathway achieves such specificity.

The major sequence of events initiated by Notch signaling is highly conserved across evolution and ultimately converges upon a single DNA binding protein, CSL, assuming an active conformation at target gene loci. CSL factors (mammalian CBF1, *Drosophila* Suppressor of Hairless, and *C. elegans* LAG-1) are the sole terminal effectors of the pathway and form a transcription-activating complex with the Notch intracellular domain during signaling (Bailey and Posakony, 1995; Christensen et al., 1996; Jarriault et al., 1995; Lecourtois and Schweisguth, 1997; Tamura et al., 1995). Since every target gene with CSL-binding sites is not ubiquitously expressed upon signaling, transcriptional regulation must be controlled to ensure that expression is specific and yields unique cell fates.

Mechanisms fine-tuning repetitive Notch signaling to establish transcriptional selectivity and define cell fates can be addressed in *C. elegans*. The LIN-12 (a Notch ortholog; hereafter referred to as LIN-12/Notch) pathway induces three distinct postembryonic cell fates during formation of a functional uterine-vulval connection required for egg laying. First, during the AC/VU decision, reciprocal signaling between two equivalent gonadal cells results in the LIN-12 signal-receiving cell adopting a ventral uterine precursor (VU) cell fate while the other cell by default becomes the terminal anchor cell (AC) (Greenwald et al., 1983; Kimble, 1981; Seydoux and Greenwald, 1989). Later, in the uterus, VU granddaughters (intermediate precursors), all expressing membrane-bound LIN-12, in closest contact with the AC expressing the membrane-bound ligand LAG-2, receive a unidirectional signal and adopt the specialized π cell fate (Newman et al., 2000; Newman et al., 1995; Wilkinson et al., 1994). Upon induction of the vulva by the AC, primary (1°) vulval cells signal adjacent vulval cells to become secondary (2°) cells, also using LIN-12 (Sternberg, 1988; Sternberg and Horvitz, 1989). Despite this repeated utilization of LIN-12 signaling, target genes expressed in the uterus may not be expressed in the vulva and vice versa. We wanted to address the mechanism(s) responsible for exclusive gene expression during LIN-12-mediated induction of the uterine π cell fate.

As a culmination of Notch signaling in π cells, the genes *egl-13*, encoding a SOX domain transcription factor, and *lin-11*, encoding a LIM domain transcription factor, are upregulated and are required for maintenance and differentiation, respectively, of the π lineage (Cinar et al., 2003; Freyd et al., 1990; Hanna-Rose and Han, 1999; Newman et al., 1999). Clusters of LAG-1 cis-elements within upstream regulatory sequences (URS) of LIN-12 target genes are a criterion for pursuing a candidate gene as a direct target of the pathway (Rebeiz et al., 2002; Yoo et al., 2004; Yu et al., 2004). Some LAG-1 binding sites present in the *lin-11* locus are sufficient to drive uterine expression, demonstrating direct regulation by LIN-12 (Gupta and Sternberg, 2002; Yoo et al., 2004). *lin-11* is also expressed in the vulva in response to Wnt activity (Gupta and Sternberg, 2002).

Unlike *lin-11*, *egl-13* is specifically expressed in the uterus and not in the vulva (Hanna-Rose and Han, 1999). We also did not detect clusters of LAG-1 binding sites in *egl-13*. Nonetheless, in this report, we establish *egl-13* as a true LIN-12 target gene. We also demonstrate the necessity of a conserved cis element for Fos and Jun transcription factors for specification stage expression of EGL-13 and rescue of mutants. Additional analyses presented here provide evidence that *fos-1*, the closest *C. elegans* homolog of Fos, is involved in π cell development and directly regulates *egl-13* expression.

MATERIALS AND METHODS

Strains

Nematode strains were handled and maintained at 20°C (Brenner, 1974). The following strains were used: wild-type strain N2 (Bristol); LGIII, *tyIs4 [egl-13^{FL}::GFP]*, *syIs80*[*lin-11::GFP* + *unc-119*(+)] (Gupta and Sternberg,

[1]Program in Developmental Biology and [2]Verna and Marrs McLean Department of Biochemistry and Molecular Biology, Baylor College of Medicine, Houston, TX 77030, USA. [3]The Honors College, Department of Biology and Biochemistry, University of Houston, Houston, TX 77204, USA.

*Author for correspondence (e-mail: apnewman@uh.edu)

Accepted 22 August 2007

2002); LG V, *fos-1(ar105)/dpy-11(e224) unc-42(e270)*, *unc-76(e911)*; LG X, *egl-13(ku194)*, *syIs123*[*fos-1a::YFP-TL* + *unc-119(+)*] (Sherwood et al., 2005). The strain *+/DnT1 IV; fos-1(ar105)/DnT1 V; syEx679[pAC-fos-1a::YFP]* (Sherwood et al., 2005) was also studied. The *tyIs4* strain is an integrated line of *egl-13^{FL}::GFP* (pWH17) (Cinar et al., 2003; Hanna-Rose and Han, 1999).

Reporter deletions

Unique restriction endonuclease sites within the pWH17 vector were used to excise intervals of *egl-13* URS. Restriction sites for deletion constructs and end point base pairs are provided in Fig. 1D. N2 hermaphrodites were injected with 20 ng/μl of each construct. The five best-transmitting extrachromosomal lines were studied.

Bioinformatics

The 6451 bp of sequence upstream to the translational start for *C. elegans egl-13* (clone T22B7.1) was obtained from the T22B7 cosmid sequence (bp 27,684-34,134; GenBank/EMBL accession no. U64608). An 8 kb genomic interval for *C. briggsae* CBG14721 was acquired from within the contig cb25.fpc3857 from assembly cb25.agp8 (bp 3,390,956-3,398,955; GenBank/EMBL accession no. CAAC01000068). Multiple (ClustalW 1.8) and pairwise (Sim) alignments were carried out using the Baylor College of Medicine Search Launcher (URL: http://searchlauncher.bcm.tmc.edu). TESS (Transcription Element Search Software, TRANSFAC database version 4.0) was utilized to identify candidate transcription factor binding sites (Schug and Overton, 1997, Technical Report CBIL-TR-1997-1001-v4.0, Computational Biology and Informatics Laboratory, School of Medicine, University of Pennsylvania; PA, USA http://www.cbil.upenn.edu/tess).

Cis-element mutagenesis

PCR-mediated, site-directed mutagenesis using overlap extension was conducted as described by Ho et al. (Ho et al., 1989). The template for mutagenesis was the *egl-13^{FL}::GFP* construct. The external oligo primers were ‘A’ (forward, 5′-GTGTCTCATCGCTCGTCAAGC-3′) and ‘D’ (reverse, 5′-CACACATACACCTGGACAAGACG-3′). The *egl-13$^{FL\Delta100bp}$::GFP* was generated using overlapping primers that removed sequence from 1325 to 1221 bp upstream of the translational start. For the LAG-1 deletion, the overlapping primer set consisted of reverse primer ‘B’ (5′-GCTGAGAAAATGGTTTTGGAAAATGTGCACTCGGTC-3′) and forward primer ‘C’ (5′-GACCGAGTGCACATTTTCCAAAACCATT-TTCTCAGC-3′). For the Fos and Jun (Fos/Jun) deletion, the overlapping primer set consisted of reverse primer ‘B’ (5′-GGCCGACCAA-AAAAAGCCGATTCACAACAATACC-3′) and forward primer ‘C’ (5′-GGTATTGTTGTGAATCGGCTTTTTTTGGTCGGCC-3′). For each deletion, two separate A plus B and C plus D PCR products were purified, combined, and added as template to a subsequent PCR reaction with A and D primers. The resulting overlap-extended products were digested with *Nar*I and *Nru*I and cloned into the *egl-13^{FL}::GFP* vector to make either *egl-13$^{\Delta LAG-1}$::GFP* or *egl-13$^{\Delta Fos/Jun}$::GFP*. For the double deletion, the same mutagenesis strategy was performed for deleting the Fos/Jun binding site but with *egl-13$^{\Delta LAG-1}$::GFP* as a template. Each construct was injected at 20 ng/μl into N2 hermaphrodites and the resulting lies used for analysis.

cDNA-mediated rescue

Full-length 1413 bp *egl-13* cDNA with a 3′ *Bam*HI site was amplified from a mixed-stage *C. elegans* cDNA library, digested with *Hin*dIII-*Bam*HI, and cloned into pPD95.69gfp(–) vector (GFP was previously removed by *Sma*I and *Eco*RI digestion and re-ligating). Then a 1.9 kb *Hin*dIII-*Aat*II fragment containing the cDNA from this intermediate GFP-minus vector was cloned into the same sites of *egl-13^{FL}::GFP* to generate *egl-13^{FL}::cDNA* (intact). A 2.5 kb *Sph*I-*Aat*II insert from *egl-13^{FL}::cDNA* was cloned into the *egl-13$^{FL\Delta LAG-1}$::GFP*, *egl-13$^{FL\Delta Fos/Jun}$::GFP*, and *egl-13$^{FL\Delta LAG-1\Delta Fos/Jun}$::GFP* recipient vectors to create respective cDNA fusions. Each was co-injected at 20 ng/μl with a *myo-2::GFP* marker at 20 ng/μl into *egl-13(ku194)* recipients. The best transmitting lines with uniform body wall GFP were studied. In Fig. 2C, data for intact lines were collected from strains *tyIs102* and *tyIs101*, ΔLAG-1 from *tyIs112* and *tyIs111*, ΔFos/Jun from *tyIs121* and *tyIs123*, and ΔLAG-1ΔFos/Jun from *tyIs132* and *tyIs133*.

RNAi

We ‘blasted’ human Fos and Jun orthologs (Fos, FOSB, FRA 1 and 2, JDP 1 and 2; Jun, JUNB, JUND; retrieved from the human protein database, www.hprd.org/) to identify similar counterparts in the *C. elegans* genome. L4 stage *tyIs4* animals were fed control (*pie-1*) or the following experimental RNAi clones from the Ahringer library (Kamath et al., 2003): F29G9.4/*fos-1*, ZK909.4, C27D6.4, F57B10.1, K08F8.2, R74.3, T24H10.7/*jun-1*, C34D1.5, and T04C10.2. W08E12.1 cDNA was amplified with 5′ *Eco*RI and 3′ *Bam*HI sites from a mixed-stage *C. elegans* cDNA library, cloned into the L4440 vector, and transformed into HT115(DE3) bacteria for testing.

Co-localization and translational fusions

We generated pPD95.69cyan and pPD95.69yfp by *Age*I-*Eco*RI dropout of GFP from pPD95.69 and replacement with either CFP from L4752 plasmid or YFP from L4753 plasmid, respectively. The *egl-13$^{1.6}$::CFP* reporter had the identical insert composition to the *egl-13$^{1.6}$::GFP* reporter, only the recipient vector in this case was pPD95.69cyan. The *plastFOS-1c::YFP* construct was created by PCR amplification of a 4.4 kb genomic fragment with 5′ *Pme*I and 3′ *Nhe*I sites (forward, 5′-CTGCAGGTTTAAACCG-TCGGCTGGGAGAAAACCTAAAG-3′; reverse, 5′-GGATCCGCTAGC-GAGTGGTCGGAGATCAGCATCCGG-3′) from the F29G9 cosmid and cloned into the *Hin*dIII(blunted)-*Xba*I-treated pPD95.69yfp vector, replacing the *fos-1* stop codon with an in-frame fusion to YFP.

Separate lines carrying one extrachromosomal array of either the *egl-13$^{1.6}$::CFP* reporter (*tyEx22*) or the *plastFOS-1c::YFP* transgene (*tyEx30* and *tyEx31*) were established in the *unc-76* background. Non-Unc (non-uncoordinated) *unc-76; Ex[plastFOS-1c::YFP(50 ng/μl) unc-76(+)(60 ng/μl)]* males were crossed into GFP-positive *unc-76; tyEx22[egl-13$^{1.6}$::CFP(20 ng/μl) rab-3::GFP(20 ng/μl)]* hermaphrodites. Phenotypically non-Unc, GFP-positive *unc-76; tyEx30* or *tyEx31[plastFOS-1c::YFP unc-76(+)];tyEx22[egl-13$^{1.6}$::CFP rab-3::GFP]* cross progeny were isolated and propagated. Three independent transgenic strains carrying both arrays were generated in this manner and found to have similar fluorescence patterns.

For the *pJUN-1d/c::GFP* translational reporter, T24H10 cosmid was digested with *Nhe*I and *Pme*I. The resulting 5293 bp (~5.3 kb) band contains 842 bp and 4266 bp of URS/intron sequence upstream of the translational starts of *jun-1d* and *jun-1c*, respectively. We cloned this fragment into *Xba*I-*Sma*I-treated pPD95.75 to establish an in-frame GFP fusion. We observed consistent expression in three extrachromosomal lines of animals expressing this reporter transgene in the *unc-76* injection system (best transmitting line is *tyEx35[pJUN-1d/c::GFP(20 ng/μl) unc-76(+)(60 ng/μl)]*).

Electrophoretic mobility shift assays

The radiolabeled probe was generated by amplification of the 100 bp homologous region within the 1.3 kb π enhancer with 5′ *Bgl*II and 3′ *Eco*RI restriction sites. The fragment was digested, de-phosphorylated, and end-labeled with [γ-^{32}P]ATP. The cDNAs for *fos-1b* and *jun-1c* engineered with 5′ *Nde*I and 3′ *Bam*HI restriction sites were amplified from a mixed-stage *C. elegans* cDNA library and cloned into pCite4a (Novagen) expression vectors. The digested *fos-1* amplicon was also cloned into the pGBKT7 (Clontech) to attach a 5′ Myc epitope tag. FOS-1 and JUN-1 proteins were then in vitro translated (Promega). For competition, forward and reverse oligonucleotides, with flanking sequences as present in *egl-13* URS, containing either intact or mutated Fos/Jun binding site were annealed. The intact sequence is 5′-GGTTGTGAATCGATTAGTCATAGATTGCTTT-3′ (the Fos/Jun binding site is underlined). The mutated sequence is 5′-GGTTGTGAATCGAgtcGTCATAGATTGCTTT-3′ (the altered Fos/Jun binding site is underlined and the mutation is in lowercase).

RESULTS

A minimal region of *egl-13* URS serves as a π-specific enhancer

Once specified from a population of twelve intermediate precursors, three π cells on each side of the ventral uterus undergo one dorsal-ventral division, distinguishable from default ρ divisions, to generate a total of 12 π cell daughters (Newman et al., 1995) (Fig. 1A).

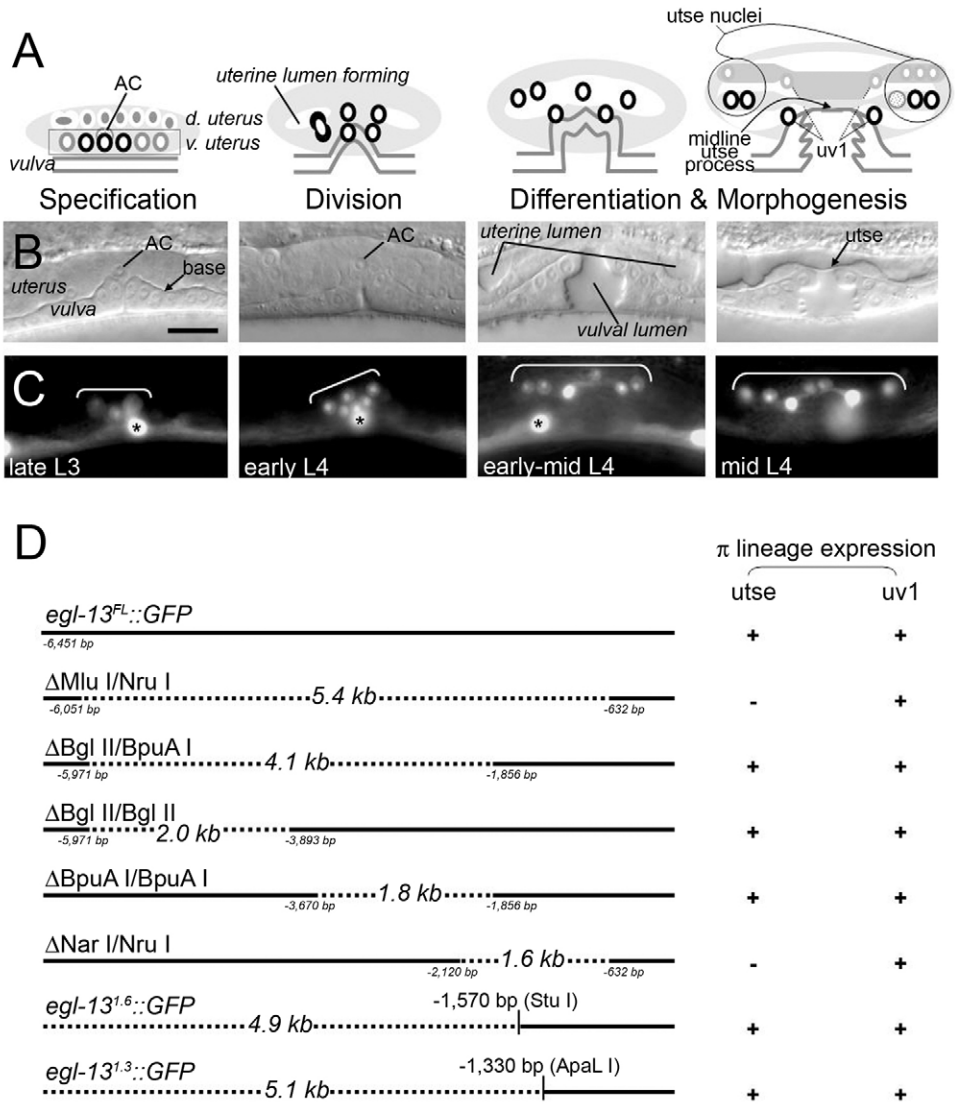

Fig. 1. A minimal 1.3 kb enhancer in *egl-13* URS drives expression specifically in the π cell lineage. (**A**) The π cells are singled out from a population of 12 VU intermediate precursors (six on one lateral side are shown, within 5 μm of the midline) surrounding the central AC, and undergo one round of cell division (d., dorsal; v., ventral). Eight π descendants plus the AC form the utse syncytium; four descendants become uv1 and are more proximal to the vulva. (**B**) Medial uterine and vulval morphology. Base, basement membrane. (**C**) In a lateral plane to B, *egl-13::GFP*(*tyIs4*) initiates uterine expression only in the π cells and persists in descendants. Fluorescent π nuclei are bracketed. Asterisks mark fluorescent nuclei of the body wall. Scale bar: 10 μm. (**D**) π lineage expression of deletion constructs generated from *egl-13^{FL}::GFP*. Restriction sites utilized, approximate deletion lengths, and end points as distances from the translational start are indicated.

Fusion among eight of the 12 daughters and the AC generates the syncytial uterine seam cell (utse). The common cytoplasm and membrane shared by this utse stretches a thin laminar process dorsal to the vulva that is first visible at the mid L4 stage and ultimately permits passage of eggs to the outside. The other four π daughters become the mononuclear uv1 cells (Newman et al., 1996) (Fig. 1A,B).

Following the specification event at the late L3 stage and just prior to division at L3 lethargus, fluorescence from an *egl-13::GFP* transcriptional reporter (pWH17) was initiated in π nuclei (Fig. 1C). Expression of this reporter, which contained 6451 bp (~6.4 kb) of *egl-13* URS, persisted through division, differentiation, and morphogenesis (Hanna-Rose and Han, 1999). The maintenance of expression throughout the lineage together with the robust upregulation in uv1 daughters suggest that the mechanisms governing *egl-13* marker expression may also be more broadly required for distinct aspects of the π cell lineage.

To resolve possible enhancers contributing to *egl-13* expression and π development, we first generated large deletions (up to ~5.4 kb) within the URS of the *egl-13::GFP* transgene and tested the remaining sequences for potential to drive π-specific expression (Fig. 1D). For the ease of following the subsequent deletions made to this full-length transgene, we refer to the *egl-13::GFP* (pWH17) reporter as *egl-13^{FL}::GFP* (FL for full length). In this manner, we were able to deduce a 1330 bp (~1.3 kb) region upstream of the translational start of *egl-13* sufficient for expressing GFP in π cells through all relevant stages of development as in Fig. 1C.

Conserved LAG-1 and Fos/Jun binding sites in the π enhancer of *egl-13* are required for expression at specification

We utilized software to predict transcription factor binding sites and performed alignments of 6.4 kb *egl-13* URS in *C. elegans* to exactly 8 kb of URS in the *Caenorhabditis briggsae* ortholog (Materials and methods). We found significant conservation of discrete stretches of sequence between the minimal 1.3 kb π enhancer of *C. elegans* to precisely 1340 bp proximal to the translational start of the *C. briggsae* ortholog (Fig. 2A).

In order to determine if the conserved sequences contribute to π-specific expression, we deleted each stretch of homologous sequence independently and in combinations and observed the uterine expression pattern from an otherwise intact *egl-13^{FL}::GFP* transgene. Pertinent to this report, we found that deletion of a 106 bp (~100 bp) homologous region at the 5′ end of the 1.3 kb π

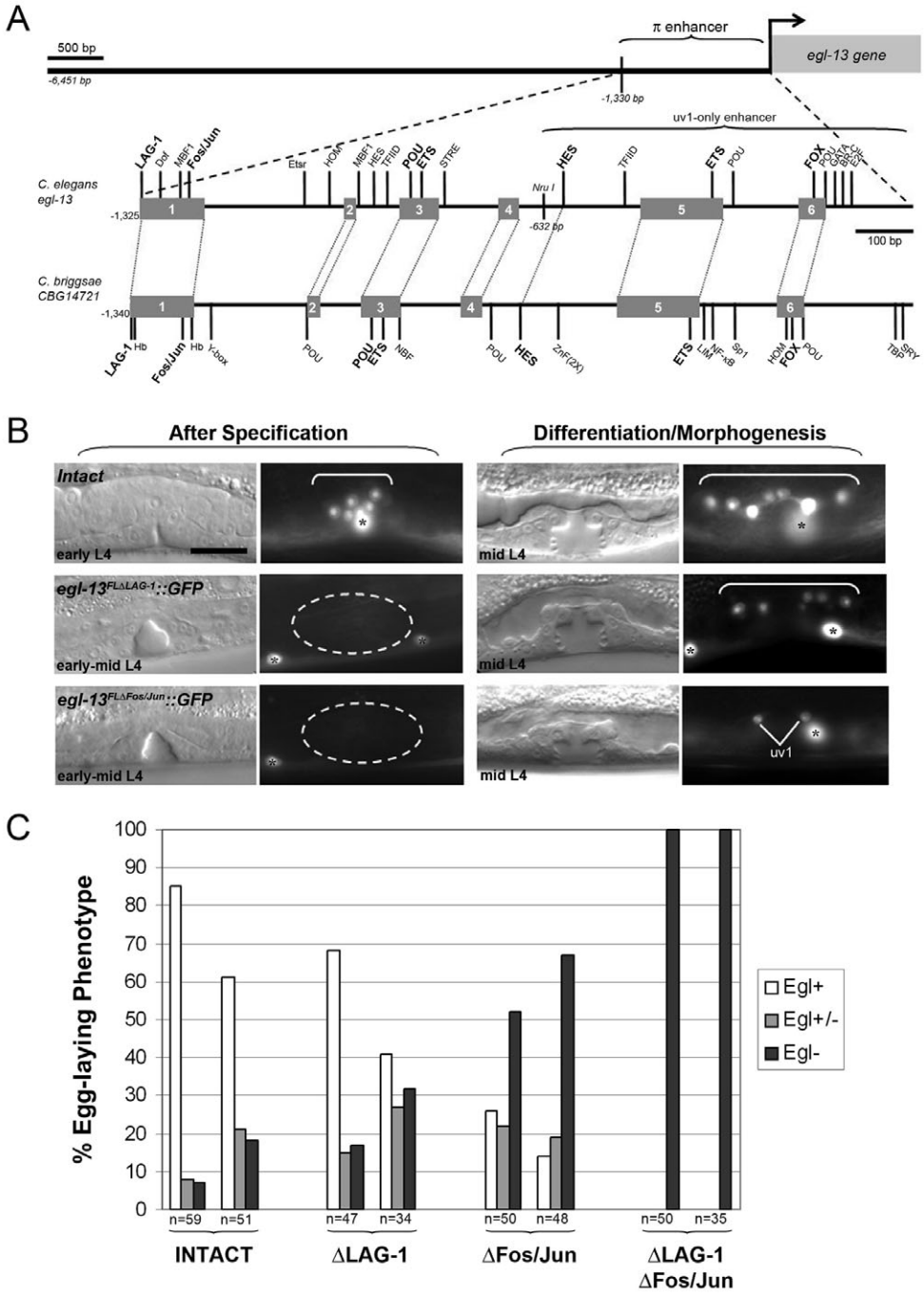

Fig. 2. LAG-1 and Fos/Jun cis binding elements are required for *egl-13* expression at π cell specification and for rescue of *egl-13* mutant defects. (**A**) Conservation of transcription factor binding sites within the 1.3 kb π enhancer of *egl-13*. Conserved cis-elements are shown in bold. Dark gray boxes represent sequences sharing remarkable identity with *C. briggsae*: 106 bp box 1 in *elegans* shares 88.2% identity with *briggsae*, 21 bp box 2 shares 100%, 65 bp box 3 shares 89.6%, 36 bp box 4 shares 94.4%, 142 bp box 5 shares 91.7%, and 45 bp box 6 shares 93.5%. Trans factor abbreviations (in order of relative upstream positions): Hb, Hunchback; Dof, Dof domain; MBF1, Multi-protein binding factor; Y-box, Y-box binding protein; Etsr, ETS domain related; HOM, homeodomain; POU, POU domain; HES, Hairy/Enhancer of split; TFIID, transcription factor II D; ETS domain; NBF, Nonamer binding protein; STRE, stress response element; ZnF, zinc finger; LIM, LIM domain; NF-κB or Rel homology; Sp1 or ZnF; FOX, F-box/Forkhead; GATA, GATA binding factor; BR-C, Broad complex or ZnF; E2F factor; TBP, TATA binding protein; SRY, SRY or high mobility group (HMG). (**B**) Effect of LAG-1 or Fos/Jun deletion on temporal uterine *egl-13*^{FL}*::GFP* fluorescence. DIC images showing medial uterine-vulval development. Lateral expression of *egl-13*^{FL}*::GFP* in π cells is seen here just after the cells have divided. Neither *egl-13*$^{FL\Delta LAG\text{-}1}$*::GFP* nor *egl-13*$^{FL\Delta Fos/Jun}$*::GFP* transgenic animals fluoresce at specification. *egl-13*$^{FL\Delta LAG\text{-}1}$*::GFP* expresses in all π descendants later, whereas later expression of *egl-13*$^{FL\Delta Fos/Jun}$*::GFP* is only in uv1. Brackets encompass the π cells. Dashed ovals surround uterine area where fluorescence is lost. Asterisks mark body wall expression. Scale bar: 10 μm. (**C**) Four constructs of *egl-13*^{FL}*::cDNA* were generated with intact, singly, or doubly-deleted LAG-1 and Fos/Jun binding sites. L4 stage hermaphrodites from independent *egl-13(ku194)* transgenic lines for each construct were scored over 4 days for egg laying. Egl+ indicates healthy appearance and egg laying. Egl+/– indicates egg laying but bloated appearance and/or rupture from internal hatching. Egl– indicates no egg laying and eventual rupture. *ku194* is 100% Egl– (*n*=100s, not shown). The strain designations are provided in Materials and methods.

enhancer (box 1 in Fig. 2A) was the only alteration that resulted in loss of tissue-specific expression in the uterus. The *egl-13$^{FL\Delta 100bp}$::GFP* showed loss of fluorescence at specification whereas later expression was retained in uv1 daughters (data not shown; Materials and methods). Expression in other tissues (body wall and neurons) was unaffected. This homologous 100 bp sequence contained two conserved binding sites: one for LAG-1 and one for basic domain leucine zipper proteins (bZIP) of the Fos and Jun (Fos/Jun) family.

In addition to the conserved, canonical LAG-1 binding site within the π enhancer, there are two additional LAG-1 binding sites, another canonical and one non-canonical, present outside the enhancer and not conserved. However, clustered LAG-1 binding sites are not apparent in the URS of either *C. elegans egl-13* or the *briggsae* ortholog. We removed the three underlined nucleotides of the conserved LAG-1 binding site 5′-GTGGGAA-3′ (the consensus sequence is 5′-RTGGGAA-3′) within the π enhancer of the full-length reporter transgene, *egl-13$^{FL\Delta LAG\text{-}1}$::GFP* (Christensen et al., 1996). This single LAG-1 deletion abolished specification stage expression of *egl-13::GFP* in the π lineage (5 lines, *n*>50 per line; Fig. 2B). Therefore, the other two LAG-1 binding sites do not play redundant roles in directing early expression. The failure of the *egl-13$^{FL\Delta LAG\text{-}1}$::GFP* construct to express GFP in the π cells at a stage concomitant with induction by LIN-12 signaling suggests that *egl-13* is a direct target of the pathway.

Deleting the conserved LAG-1 binding site affected early π expression; however, later expression in the differentiated utse and uv1 daughters was resumed. We reasoned that an additional cis element in the 100 bp homologous region must be driving later utse expression, which was absent when the entire region was removed. Thus, we deleted the Fos/Jun binding site to generate *egl-13$^{FL\Delta Fos/Jun}$::GFP*. Similar to deletion of the single LAG-1 site, deletion of the Fos/Jun site abolished expression at π specification (5 lines, *n*>50 per line; Fig. 2B). However, unlike the LAG-1 deletion, later utse expression was also compromised, resembling the expression pattern observed for *egl-13$^{FL\Delta 100bp}$::GFP*. We infer that the conserved Fos/Jun binding site is equally crucial to the LAG-1 site for expression of *egl-13* at specification and independently required for expression in π daughters that differentiate into utse cells.

LAG-1 and Fos/Jun cis elements are required for rescue of *egl-13* mutants

Homozygous *egl-13(0)* mutants do not lay eggs. As a consequence, the hermaphrodite is consumed by internally-hatched larva and becomes a ‘bag of worms’ (Hanna-Rose and Han, 1999; Trent et al., 1983). This egg-laying-defective phenotype is presumably caused by an earlier malformation of the utse, such that the uterine-vulval junction is blocked with thick tissue and an unfused AC (Cinar et al., 2003; Hanna-Rose and Han, 1999).

Normal egg laying can be restored in *egl-13* mutants by exogenous delivery of *egl-13* genomic or cDNA coding sequences (Hanna-Rose and Han, 1999). We tested if the LAG-1 and Fos/Jun sites that are crucial for proper expression were required for rescue of *egl-13* null mutants (Fig. 2C). We made four versions of full-length URS driving *egl-13* cDNA expression: one *egl-13^{FL}::cDNA* (intact) and three with either the LAG-1, Fos/Jun or both binding sites deleted. First, we established that the intact construct could rescue transgenic lines of *egl-13(ku194)*. We found that over-expression of *egl-13* cDNA from the *egl-13$^{FL\Delta LAG\text{-}1}$::cDNA* construct was also sufficient to restore egg-laying ability. The rescue conferred by over-expression of *egl-13$^{FL\Delta Fos/Jun}$::cDNA* was significantly less but not absent. However, when both sites were deleted to generate *egl-13$^{FL\Delta LAG\text{-}1\Delta Fos/Jun}$::cDNA*, no rescue of egg-laying defects was achieved. Two lines of *egl-13$^{FL\Delta LAG\text{-}1\Delta Fos/Jun}$::cDNA* in an additional *egl-13* null allele, *ty3*, also remained completely egg-laying defective (*n*=24 and *n*=25).

fos-1 mutants have uterine defects and fail to express π-specific markers

The nonconsensus bZIP binding site, 5′-TTAGTCA-3′, in the π enhancer is more similar to the consensus binding site for Fos and Jun, 5′-TGA(C/G)TCA-3′, than to other subclasses of bZIP transcription factors (Angel et al., 1987; Lee et al., 1987). We retrieved *fos-1* and T24H10.7, sharing 33% and 41% identity, respectively, in their functional bZIP domains, as the closest *C. elegans* homologs to the mammalian oncogenes c-Fos and c-Jun, respectively. In this section, we address the role of *fos-1* in the uterus. Later in this report, we provide the first documentation of an in vitro biological activity and tissue localization for T24H10.7, now referred to as *jun-1*.

We examined genetic *fos-1(ar105)* mutants (Seydoux et al., 1993; Sherwood et al., 2005) and found that they consistently lack an apparent uterine lumen and a utse-like process (Fig. 3A). We also noted the absence of uterine *egl-13::GFP* fluorescence in *ar105* from specification through later L4 stages, whereas body wall fluorescence was unaffected (Fig. 3A).

The sequence alteration in *fos-1(ar105)* leads to a nonsense mutation truncating the *fos-1a* transcript; however, generation of other functional bZIP-containing transcripts, such as *fos-1b*, is not perturbed (Sherwood et al., 2005) (Fig. 5A). To evaluate the consequences of eliminating all isoforms, we performed RNAi to *fos-1* in the *tyIs4* background using a sequence that specifically targets the functional leucine zipper (dimerization) domain. The L4 stage undifferentiated uterus and loss of uterine *egl-13::GFP* fluorescence in *fos-1* RNAi-treated animals were indistinguishable from those in *ar105* animals (Fig. 3B). In later adult stages, *fos-1(ar105)* and *fos-1(RNAi)* animals displayed protruding vulva (Pvul) phenotypes, typical of uterine-vulval abnormalities. In addition, both *fos-1(ar105)* and *fos-1(RNAi)* are completely penetrant for sterility (Ste). The fact that the *fos-1(RNAi)* uterine phenotype closely resembles but is not worse than that of *fos-1(ar105)* suggests that the *fos-1a* isoform could specifically play the earliest role in uterine development.

We also investigated whether *lin-11*, an additional π marker, is expressed in *fos-1* mutants. Expression of *lin-11* in π cells is directly regulated by LIN-12 signaling, whereas expression in the vulva is regulated by Wnt signaling (Gupta and Sternberg, 2002). We compared the dynamic expression of a *lin-11::GFP* reporter during uterine-vulval development in the *fos-1(ar105)* background with the wild type (Fig. 4). We did not detect uterine *lin-11* fluorescence at π cell specification or later relevant stages in *fos-1* mutants (Fig. 4C-D,L for the wild type, Fig. 4G-H,Q for *ar105*). Conversely, we observed appropriate *lin-11* expression in the 2° vulval lineage in *fos-1* mutants (Fig. 4E-F,N-R) as in the wild type (Fig. 4A-B,I-M).

The AC in *fos-1(ar105)* fails to invade underlying primary vulval tissue during L3 stage uterine development, a process integral in securing proper orientation of the uterine-vulval connection (Sherwood et al., 2005; Sherwood and Sternberg, 2003). By showing that specifically driving *fos-1a* cDNA expression in the AC was sufficient to restore AC invasion, Sherwood et al. concluded that FOS-1a probably facilitates the expression of genes required to

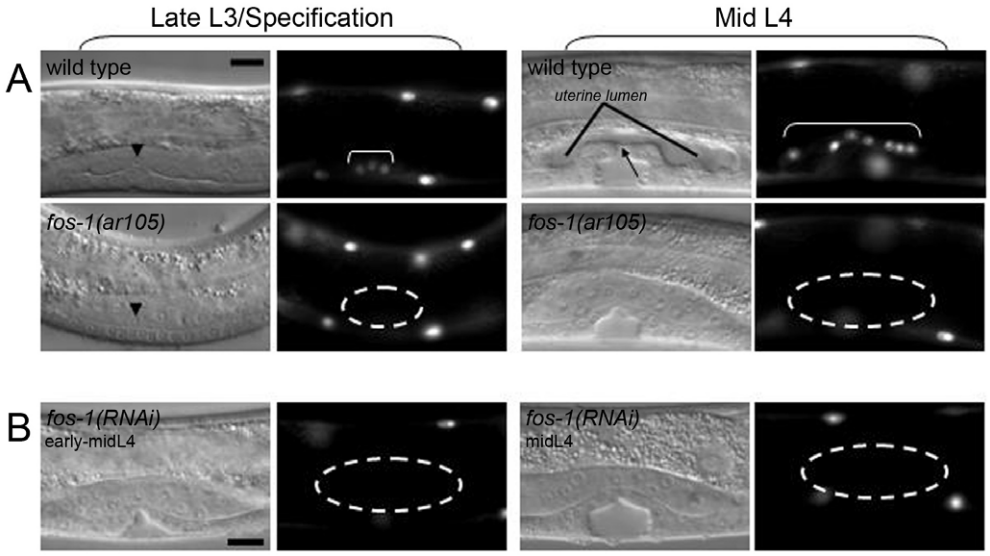

Fig. 3. *fos-1* loss-of-function causes abnormal uterine morphology and absence of uterine *egl-13* expression. (**A**) Specification and mid L4 stage expression of *egl-13::GFP(tyIs4)* in the wild type and *fos-1(ar105)*. *fos-1(ar105)* do not express GFP in uterine tissue (dashed ovals indicate where fluorescence was expected; fluorescent π nuclei in the wild type are bracketed). The mid L4 stage uterus in *ar105* is undifferentiated by comparison with the wild type, as apparent by the absence of a uterine lumen. Arrow indicates the utse, observed only in the wild type. Other GFP-positive cell bodies belong to the body wall, where fluorescence is not affected. (**B**) No uterine *egl-13::GFP* expression or lumen is observed after *fos-1* RNAi treatment. Scale bar: 10 μm.

bestow invasive properties on the AC (Sherwood et al., 2005). We further examined a line rescued for FOS-1A activity in the AC only (Materials and methods) and found that uterine defects persisted regardless of a presumably normal AC (*n*=35 mid L4 stage animals, data not shown). We infer that AC invasion is not the only process impaired by loss of *fos-1a* function and that the AC is not the only uterine cell that requires *fos-1*. Rather, *fos-1a* appears to function independently and autonomously in uterine cells.

FOS-1 is expressed in all precursor cells that can adopt the π cell fate

Studies with *fos-1* reporter fusions resolved that *fos-1a* and *fos-1b* transcripts are expressed throughout the uterus during gonadogenesis (Sherwood et al., 2005). We observed that a *fos-1a* translational fusion is expressed throughout the VU intermediate prescursor cells, including π cells, a pattern consistent with loss of *fos-1a* in *ar105* failing to give rise to π-derived tissue (data not shown). To better resolve precise uterine expression, we cloned smaller pieces of the *fos-1* locus that might potentially contain a uterine enhancer separated from other gonadal enhancers (Sherwood et al., 2005). We observed uterine-specific expression from a translational fusion which we refer to as *plastFOS-1c::YFP*. This 4.4 kb genomic construct includes an approximately ~2 kb intron preceding the last four exons and may represent the shortest bZIP-encoding FOS-1 isoform, or *fos-1c* (Fig. 5A). *plastFOS-1c::YFP* showed expression primarily in the early dorsal and ventral uterus during L3 and L4 stages. Importantly, we observed expression in all VU intermediate precursors including π cells (Fig. 5B-D). Furthermore, we confirmed that *plastFOS-1c::YFP* co-localized with cells expressing an *egl-13* π marker from the late L3 induction stage (Fig. 5D-F) through generation of π descendants (Fig. 5G-J).

plastFOS-1c::YFP may represent a downstream uterine enhancer directing expression of the characterized isoforms. However, our lab has documented that large introns within a locus can function as separate promoters for transcription of other often differentially expressed isoforms in *C. elegans* (Choi and Newman, 2006). Based on the presence of a predicted promoter region, conserved proximal TATA box, in-frame translational START codon (ATG), and identification of this specific isoform as the closest *C. briggsae* homolog, we suggest that *fos-1c* may be a unique product of the *C. elegans fos-1* gene. Since the only genetic mutant of *fos-1* specifically affects *fos-1a* and has broad uterine defects, we could not readily assess the relative contributions of *fos-1a*, *b* or *c* to the specific process of π cell induction.

FOS-1 specifically binds in vitro to *egl-13* URS as a heterodimer with JUN-1

Fos proteins form less stable homodimers than Jun and generally function as heterodimers with Jun (O'Shea et al., 1992). Nonetheless, we tested if FOS-1 as a homodimer can directly bind target sequence in a novel manner in *C. elegans*. We performed electrophoretic mobility shift assays (EMSA) with the 100 bp homologous region of *egl-13* URS (box 1, Fig. 2A). This radiolabled probe containing the conserved Fos/Jun binding site failed to produce a shifted band in the presence of in vitro translated FOS-1 alone or JUN-1 alone (Fig. 6, first gel, lane 2 and 3, respectively).

The consensus seven base pair binding site 5′-TGA(C/G)TCA-3′ for Fos/Jun binding is palindromic from the central C or G base pair and results in two asymmetric half-sites 5′-TGAC-3′ and 5′-TGAG-3′ which facilitates Fos/Jun heterodimer or Jun dimer binding (Glover and Harrison, 1995). The nonconsensus binding site 5′-TTAGTCA-3′ in *egl-13*, with one nonconsensus half site, 5′-TTAG-3′, and one consensus half site, 5′-TGAC-3′, may favor binding by a Fos/Jun heterodimer (Ramirez-Carrozzi and Kerppola, 2003). Thus, we tested if FOS-1 and JUN-1 together can bind *egl-13* URS in vitro. Indeed, we observed a striking band shift in the presence of both FOS-1 and JUN-1 (Fig. 6A, first gel, lane 4). We also observed a prominent supershift when we added antibody against Myc to the reaction, demonstrating that the shifted complex specifically included a recombinant N-terminal Myc-tagged version of FOS-1

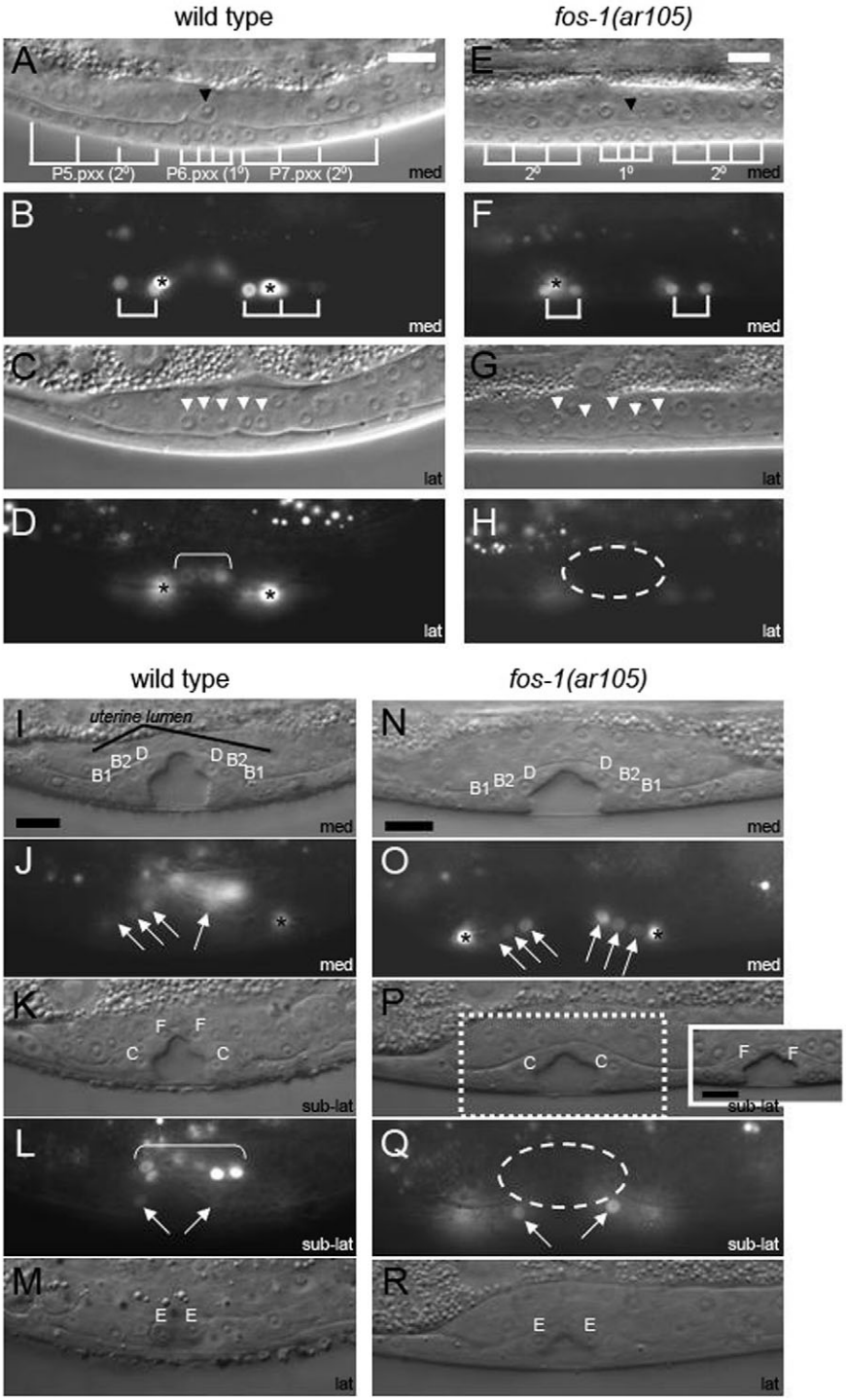

Fig. 4. *fos-1* function is required for uterine but dispensable for vulval expression of *lin-11*. (**A-H**) Comparison of late L3 stage *lin-11::GFP*(*syIs80*) expression in the wild type and *fos-1(ar105)*. (A,B) In the medial plane (med) of the wild type, *lin-11* expression is observed in the 2° vulval cells closest to the 1° vulval cells. (C,D) In the lateral plane (lat) of the wild type, out of the five VU intermediate precursors, *lin-11* is expressed in the three π cells. In the medial plane of *fos-1*, *lin-11* is also expressed in 2° vulval cells (E,F); however, laterally, *lin-11* expression is absent in the uterus (G,H). (**I-R**) Early to mid L4 stage expression of *lin-11::GFP* in the wild type and *fos-1(ar105)*. 1° vulval cells, vulF and vulE, and 2° vulval cells, vulD, vulC, vulB2 and vulB1, are indicated. In the medial (I,J) and sub-lateral (sub-lat, K,L) planes of the wild type, terminal descendants of the 2° vulval lineage continue to express *lin-11*. Expression is also detected in π descendants (L). In the medial (N,O) and sub-lateral (P,Q) planes of *fos-1*, *lin-11* expression is appropriately detected in the 2° lineage. However, no uterine *lin-11* expression is observed (Q). Black arrowheads point to the AC. White arrowheads point to uterine intermediate precursor cells. In A,B and E,F, brackets indicate vulval cells; elsewhere, brackets indicate π cells. Dashed ovals surround uterine area where fluorescence is lost. White arrows point to GFP+ 2° vulval cell descendants. Asterisks mark expression in VC neurons. Scattered background signals are from gut autofluorescence. Scale bar: 10 μm.

(Fig. 6A, first gel, lanes 5 and 6). Addition of intact but not mutated unlabeled templates significantly reduced the supershift (Fig. 6A, second gel).

These results support *egl-13* being a direct target of FOS-1 regulation through an obligate heterodimer with JUN-1 in vitro. We performed RNAi to *jun-1* but did not discern any phenotypes similar to *fos-1* knockdown. We then conducted blast searches of mammalian Fos and Jun proteins against the *C. elegans* genome to find additional paralogs to test (Materials and methods). After several rounds of single, and in combination with *jun-1(RNAi)*, feeding experiments, we were still not able to detect uterine phenotypes or loss of uterine *egl-13::GFP* upon performing RNAi to other candidates. Our inability to detect a loss-of-function phenotype could be due to redundancy in the system or lack of effectiveness of RNAi.

VU intermediate precursors express JUN-1

The above biochemical data prompted us to determine whether *jun-1* is expressed in the uterus at the appropriate time to be operative in π cell specification. First, we generated a transcriptional reporter of ~5 kb of URS ahead of the first exon fused to GFP. In five independently generated lines, we observed diffuse transgene expression throughout

the animal; however, we could not detect specific uterine expression (data not shown). Therefore, as with our analysis of a more specific uterine enhancer in the *fos-1* locus, we sought to determine if such tissue-specific drivers are present within the ~19 kb *jun-1* locus. After testing several reporter fusions, our best inference of uterine *jun-1* expression came from a genomic translational reporter which we refer to as *pJUN-1d/c::GFP* (Fig. 6B). We observed expression of *pJUN-1d/c::GFP* in the AC and surrounding VU intermediate precursors at the time of π cell specification (Fig. 6C-F). Interestingly, translational reporters of *fos-1a*, *b* and *c* and here *jun-1* display indistinguishable expression throughout dorsal and ventral uterine cells at the late L3 stage (this study) (Sherwood et al., 2005). Taken together with the loss of differentiated uterine structures in L4 stage *fos-1(ar105)* mutants, we suggest that Fos/Jun heterodimeric regulation may be a plausible facet of proper uterine development.

DISCUSSION

Fos activity is required for π cell potential

We elucidated a novel regulatory interaction between LIN-12/Notch and FOS-1 to establish the uterine π cell fate and promote expression of a downstream gene. We found that independent deletions to conserved LAG-1 or Fos/Jun cis-regulatory elements compromised expression of *egl-13* at specification. Deletion of both sites negated transgenic rescue of *egl-13* mutants. We observed that uterine tissue of *fos-1*-deficient animals appeared undifferentiated and did not give rise to structural features such as a utse or lumen. In addition, uterine expression of *egl-13* and *lin-11* markers was specifically lost in *fos-1* mutants. We also demonstrated that *fos-1* is uniformly expressed in the VU lineage including the π cells at the time of specification. Together, our results suggest that *fos-1* is broadly required for uterine development, and it also functions more specifically in π cell induction and *egl-13* expression.

Unlike *lin-12*, *fos-1* had not previously been implicated in π fate specification. Prior study has shown that all VU granddaughters have an intrinsic ability to adopt π-like fates in the presence of constitutive LIN-12 activity, which bypasses the required cell-cell interactions with the signal-presenting AC (Newman et al., 1995). By contrast, LIN-12 signaling in other tissues results in other outcomes. Here we suggest that FOS-1 activity in the early ventral uterus is one mechanism by which progenitors are instilled with the unique potential to adopt the π cell fate. Specifically, we have shown that transcriptional regulation of the LIN-12 target gene *egl-13*

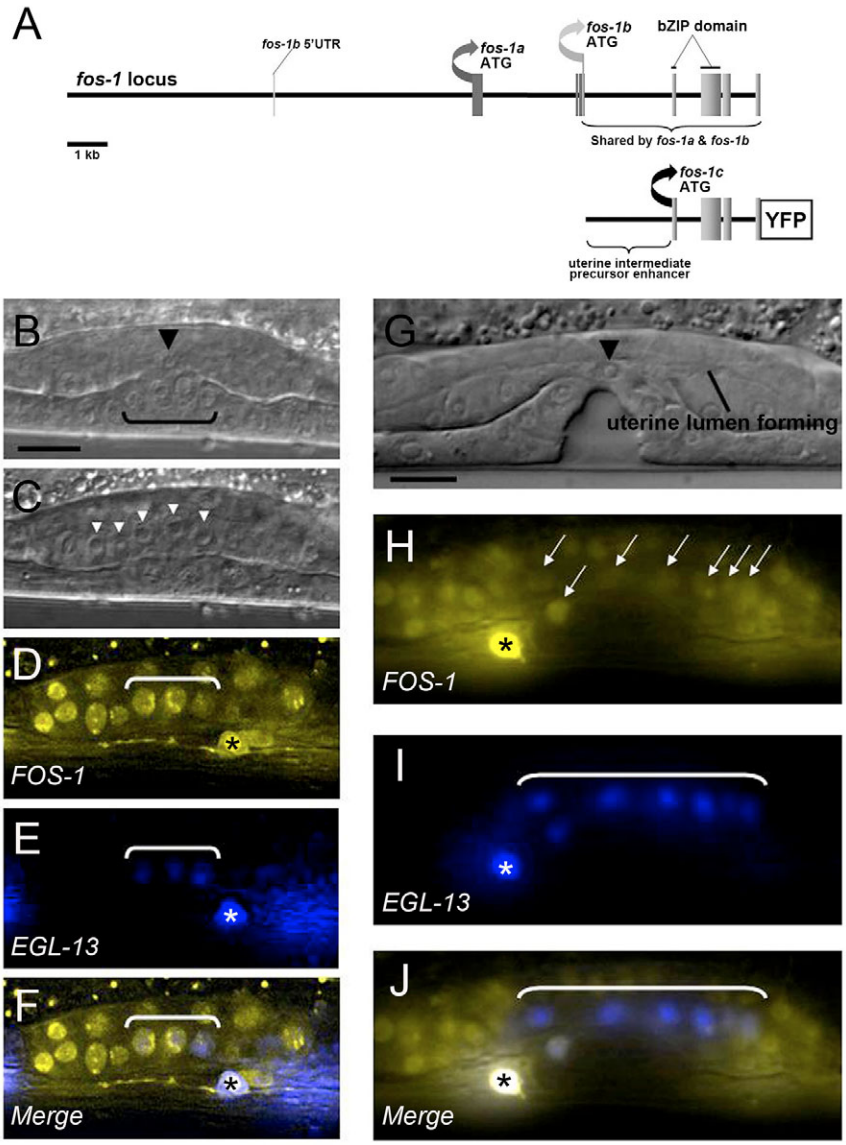

Fig. 5. FOS-1 is expressed in the intermediate precursors and co-localizes with EGL-13 during the π lineage. (**A**) *fos-1* locus with isoform *a*, *b*, and putative *c* translational starts and origin of *plastFOS-1c::YFP* indicated. (**B-F**) Late L3 stage. (B) The AC (black arrowhead) is invading underlying primary vulval cells (black bracket). (D) Approximately 5 μm from B, FOS-1c is expressed in all dorsal and ventral uterine cells including the VU intermediate precursors (C, white arrowheads). (E) Three π cells express *egl-13::CFP* (white bracket). (F) Merged image of D and E showing that FOS-1c co-localizes with *egl-13* at specification. (**G-J**) Mid L4 stage. (H) FOS-1c is broadly expressed in numerous uterine cells. White arrows point to six π cell daughters plus the AC. (I) π descendants continue to express *egl-13::CFP*. (J) Merged image of H and I showing FOS-1c also co-localizes to the π descendants. Asterisks mark non-specific fluorescence from the GFP co-transformation marker. Scale bar: 10 μm.

necessitates synergy with Fos activity. The overlap of these two pathways could be a critical link that sets specification of π cells apart from other Notch-mediated decisions. This conclusion is supported by our finding that loss of *fos-1* did not alter specification of the 2° vulval cells, another well-characterized LIN-12-induced lineage, as evident by the appropriate expression of a 2° marker in this tissue.

We show that FOS-1 can specifically bind to *egl-13* URS as an evolutionarily conserved heterodimer with JUN-1. The lack of a *jun-1* RNAi phenotype suggests that perhaps FOS-1 alone could regulate *egl-13* in vivo or that other Jun-like proteins could functionally substitute as competent partners for FOS-1. The latter redundancy of Jun activity has been observed in mammalian systems (Mechta-Grigoriou et al., 2001). Our expression analysis suggests a role for *jun-1* in uterine development.

EGL-13 expression relies on dual cis-regulation by LAG-1 and Fos/Jun

Deletion of the conserved LAG-1 and Fos/Jun-binding sites indicated that both are required for *egl-13* expression at specification, whereas Fos/Jun, but not LAG-1, is required later in the lineage. The Fos/Jun pathway may also regulate the development of π cell descendants, perhaps by promoting expression of *egl-13* and other critical factors. Our studies also revealed the presence of a uv1-specific enhancer.

Mutant rescue by over-expressing *egl-13* cDNA behind intact or ablated cis-elements gave results that were consistent with those above. Use of a rescue construct with a LAG-1 deletion resulted in a range of egg-laying ability – from comparable to intact to more attenuated. The presumptive π cells of *egl-13* mutants initiate the appropriate division pattern before abnormally dividing again (Cinar

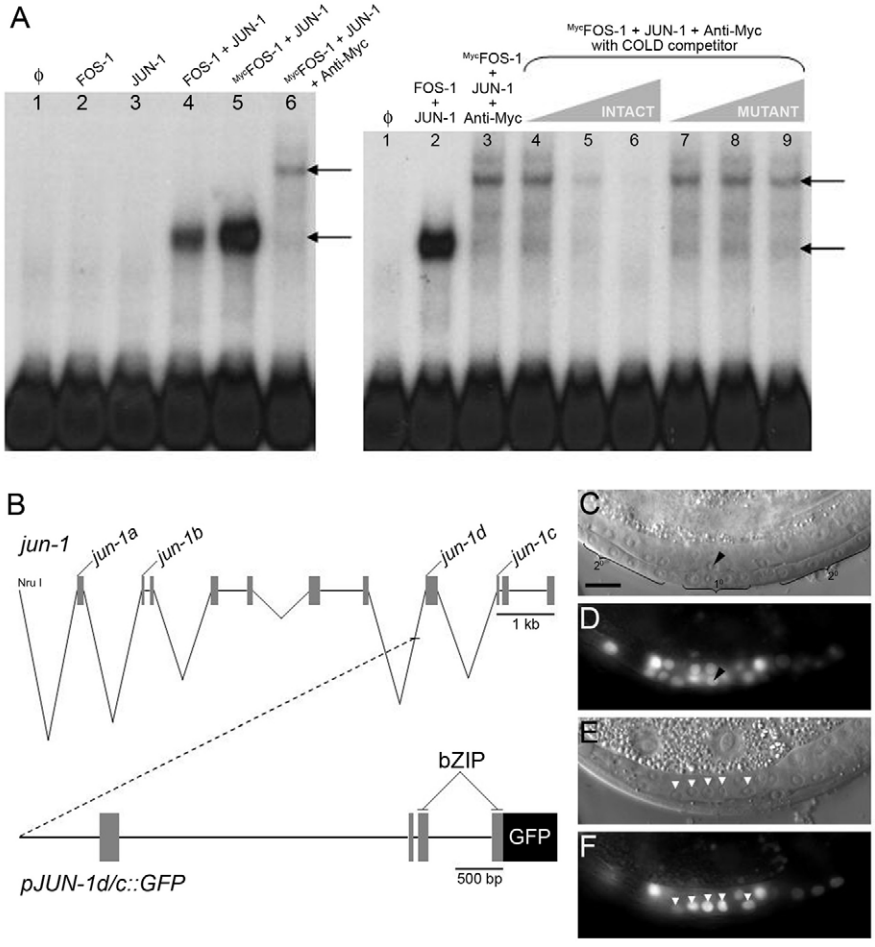

Fig. 6. FOS-1 can directly bind to *egl-13* URS as a heterodimer with JUN-1, which is also expressed throughout the uterus at π cell specification. (**A**) EMSA with labeled 100 bp homologous template containing the Fos/Jun binding site. Left gel: No band shift was detected with only lysate present (ϕ, lane 1), FOS-1 alone (lane 2), or JUN-1 alone (lane 3). A shifted complex (bottom arrow) was observed in the presence of both FOS-1 and JUN-1 (lane 4) and also with a Myc-tagged version of FOS-1 with JUN-1 (lane 5). Addition of polyclonal anti-Myc antibody in lane 6 produced a supershift due to increase in molecular mass of DNA-protein complex plus Ab (top arrow) and also completely neutralized the original band shift (bottom arrow) due to titration of protein from forming a stable complex. Right gel: The supershift was significantly reduced in the presence of unlabeled (COLD) sequence containing the *egl-13* Fos/Jun binding site (lanes 4-6) but not effectively reduced by an excess of unlabeled sequence carrying a mutated Fos/Jun binding site (lanes 7-9). Gray triangles above lanes 4-6 and 7-9 represent increasing amounts (5×, 25× and 125×, respectively) of unlabeled 30 bp competitor oligonucleotides. (**B**) This diagram represents the position of the isolated 5.3 kb genomic sequence in *pJUN-d/c::GFP* in the context of the entire *jun-1* locus. The *Nru*I site is a starting reference point for ~5 kb upstream of the first transcript. The translational starts for verified isoforms are indicated. (**C-F**) Uterine JUN-1 expression. (C,D) In the medial plane, expression of *pJUN-d/c::GFP* is detected in the AC (black arrowhead) as well as throughout the dorsal and ventral uterus. (E,F) In a lateral plane, VU intermediate precursors (white arrowheads) also express the translational reporter. Scale bar: 10 μm.

et al., 2003; Hanna-Rose and Han, 1999). For that reason, we infer that the function of EGL-13 is not required for the earliest aspects of the lineage. Thus, the extent of egg laying restored by the LAG-1 deletion construct may reflect *egl-13* expression that is early enough to effectively maintain the lineage.

The more attenuated rescue by the Fos/Jun deletion construct is consistent with a more pronounced loss of *egl-13* expression early and later in the π lineage. Yet, how can we account for the 20-30% of mutants completely rescued? First, weak fluorescence signals emitted by reporter fusion lines may be undetectable. Also, each single deletion rescue transgene at high-copy in a non-chromosomal context may be able to recruit transcriptional machinery and activate gene expression on its own. Therefore, cumulative, albeit low grade, permissive expression may provide sufficient EGL-13 activity to reinstate π cell development in single site-deleted rescue lines and account for the completely rescued mutants.

Nonetheless, the fact that mutant transgenic lines remained completely Egl when both LAG-1 and Fos/Jun binding sites were omitted from the rescue construct reinforces the importance of these sites. Our data suggests that transcriptional machinery cannot be recruited to activate *egl-13* expression at specification of the uterine π cell fate in the absence of both conserved LAG-1 and Fos/Jun cis-elements, which are apparently not required for expression in other cells. We propose that regulation by LIN-12 and Fos/Jun largely governs whether *egl-13* and perhaps other uncharacterized LIN-12/Notch target genes are expressed during uterine development.

Tissue-specific expression of *egl-13* during π cell development

Clustered LAG-1 binding sites are a hallmark of many Notch-regulated genes. Previously, direct target genes of LIN-12/Notch signaling were predicted by in silico approaches scouting for numerous LAG-1 binding sites distributed throughout the genome (Rebeiz et al., 2002; Yoo et al., 2004; Yu et al., 2004). However, one or a few LAG-1 binding sites may be crucial (Kim et al., 1996), even in genes with multiple such sites (Christensen et al., 1996; Gupta and Sternberg, 2002; Wilkinson et al., 1994). Our findings highlight that one functional LAG-1 cis-element in conjunction with an additional element for another transcription factor or pathway can direct tissue-specific expression of a LIN-12 target gene. Such combinatorial control of Notch target gene regulation has been documented in *Drosophila* (Cave et al., 2005).

Relevant to our report, *egl-43*, a zinc finger transcription factor, contains multiple LAG-1 regulatory sites and is implicated in π cell development (Hwang et al., 2007; Rimann and Hajnal, 2007). Attenuated expression of π-specific markers and malformation of utse were observed in the absence of *egl-43* via RNAi treatment (Rimann and Hajnal, 2007). In contrast to the LIN-12 target genes *egl-13* and *lin-11*, which are expressed in just the π lineage, *egl-43* expression was observed more broadly (Hwang et al., 2007; Rimann and Hajnal, 2007). Epistasis experiments suggested that *egl-43* acted downstream of, or in parallel to, *lin-12*. Since *egl-43* appears to be involved in π cell fate specification (Rimann and Hajnal, 2007) whereas *egl-13* is required for π cell fate maintenance (Cinar et al., 2003), it is possible that *egl-43* acts between *lin-12* and *egl-13*. Our studies demonstrate that *egl-13* is a direct target of *lin-12* as well as of *fos-1*; however, *egl-13* may also be regulated, either directly or indirectly, by *egl-43*.

Notch and Fos/Jun, an evolving relationship

The 100 bp interval containing the critical LAG-1 and Fos/Jun binding sites in the π enhancer of *C. elegans egl-13* has ~90% identity to the homologous interval in *C. briggsae* and is located at an equivalent upstream distance in each ortholog. Such accurate conservation after 100 million years of divergence suggests the importance of this cis-regulatory module. Intriguingly, this motif may represent a transcription code mandating cooperation between activating complexes recruited by the NICD-LAG-1 complex and FOS-1 heterodimer. Such models of synergy among associated DNA binding proteins at discrete enhancers have been documented as underlying mechanisms for tissue-specific gene expression.

In a broader scope, Notch and Fos/Jun pathways are both involved in major events such as T cell development and cancer progression (Foletta et al., 1998; Radtke et al., 2004; Tulchinsky, 2000; Vogt, 2001; Weng and Aster, 2004). Many lines of evidence put Notch and Fos/Jun activity at close range, including recent studies of the *egl-43* gene in *C. elegans* (Hwang et al., 2007; Rimann and Hajnal, 2007). However, our study is the first to expose a cooperative and compulsory interaction between them. Considering the widely implemented and highly conserved nature of Notch and Fos/Jun signaling pathways, we speculate that such synergistic communication of the two may be present in higher order systems as well.

We thank the CGC, Sanger Center, Dave Sherwood, and Barbara Perry for strains and clones and Wendy Hanna-Rose for pWH17. We appreciate the very helpful discussions with Jaebok Choi, Xiaohong Leng, and Melih Acar. We are grateful to the laboratories of Zheng Zhou and Tae Ho Shin for technical advice and reagents as well as Xiangwei He, Richard Atkinson, and Victor Venegas for assistance with imaging. W also thank the Baylor Department of Biochemistry for their generous support. This work was funded by the National Institute of Environmental Health Sciences (NIEHS) training grant no. T32 ES07332 to K.S.O. and by grants from the Alzheimer's Association and the NIH to A.P.N.

References

Angel, P., Imagawa, M., Chiu, R., Stein, B., Imbra, R. J., Rahmsdorf, H. J., Jonat, C., Herrlich, P. and Karin, M. (1987). Phorbol ester-inducible genes contain a common cis element recognized by a TPA-modulated trans-acting factor. *Cell* **49**, 729-739.

Bailey, A. M. and Posakony, J. W. (1995). Suppressor of hairless directly activates transcription of enhancer of split complex genes in response to Notch receptor activity. *Genes Dev.* **9**, 2609-2622.

Brenner, S. (1974). The genetics of Caenorhabditis elegans. *Genetics* **77**, 71-94.

Cave, J. W., Loh, F., Surpris, J. W., Xia, L. and Caudy, M. A. (2005). A DNA transcription code for cell-specific gene activation by notch signaling. *Curr. Biol.* **15**, 94-104.

Choi, J. and Newman, A. P. (2006). A two-promoter system of gene expression in C. elegans. *Dev. Biol.* **296**, 537-544.

Christensen, S., Kodoyianni, V., Bosenberg, M., Friedman, L. and Kimble, J. (1996). lag-1, a gene required for lin-12 and glp-1 signaling in Caenorhabditis elegans, is homologous to human CBF1 and *Drosophila* Su(H). *Development* **122**, 1373-1383.

Cinar, H. N., Richards, K. L., Oommen, K. S. and Newman, A. P. (2003). The EGL-13 SOX domain transcription factor affects the uterine pi cell lineages in Caenorhabditis elegans. *Genetics* **165**, 1623-1628.

Foletta, V. C., Segal, D. H. and Cohen, D. R. (1998). Transcriptional regulation in the immune system: all roads lead to AP-1. *J. Leukoc. Biol.* **63**, 139-152.

Freyd, G., Kim, S. K. and Horvitz, H. R. (1990). Novel cysteine-rich motif and homeodomain in the product of the Caenorhabditis elegans cell lineage gene lin-11. *Nature* **344**, 876-879.

Glover, J. N. and Harrison, S. C. (1995). Crystal structure of the heterodimeric bZIP transcription factor c-Fos-c-Jun bound to DNA. *Nature* **373**, 257-261.

Greenwald, I. S., Sternberg, P. W. and Horvitz, H. R. (1983). The lin-12 locus specifies cell fates in Caenorhabditis elegans. *Cell* **34**, 435-444.

Gupta, B. P. and Sternberg, P. W. (2002). Tissue-specific regulation of the LIM homeobox gene lin-11 during development of the Caenorhabditis elegans egg-laying system. *Dev. Biol.* **247**, 102-115.

Hanna-Rose, W. and Han, M. (1999). COG-2, a sox domain protein necessary for establishing a functional vulval-uterine connection in *Caenorhabditis elegans*. *Development* **126**, 169-179.

Ho, S. N., Hunt, H. D., Horton, R. M., Pullen, J. K. and Pease, L. R. (1989). Site-directed mutagenesis by overlap extension using the polymerase chain reaction. *Gene* **77**, 51-59.

Hwang, B. J., Meruelo, A. D. and Sternberg, P. W. (2007). C. elegans EVI1 proto-oncogene, EGL-43, is necessary for Notch-mediated cell fate specification and regulates cell invasion. *Development* **134**, 669-679.

Jarriault, S., Brou, C., Logeat, F., Schroeter, E. H., Kopan, R. and Israel, A. (1995). Signalling downstream of activated mammalian Notch. *Nature* **377**, 355-358.
Kamath, R. S., Fraser, A. G., Dong, Y., Poulin, G., Durbin, R., Gotta, M., Kanapin, A., Le Bot, N., Moreno, S., Sohrmann, M. et al. (2003). Systematic functional analysis of the Caenorhabditis elegans genome using RNAi. *Nature* **421**, 231-237.
Kim, J., Sebring, A., Esch, J. J., Kraus, M. E., Vorwerk, K., Magee, J. and Carroll, S. B. (1996). Integration of positional signals and regulation of wing formation and identity by Drosophila vestigial gene. *Nature* **382**, 133-138.
Kimble, J. (1981). Alterations in cell lineage following laser ablation of cells in the somatic gonad of Caenorhabditis elegans. *Dev. Biol.* **87**, 286-300.
Lecourtois, M. and Schweisguth, F. (1997). Role of suppressor of hairless in the delta-activated Notch signaling pathway. *Perspect. Dev. Neurobiol.* **4**, 305-311.
Lee, W., Mitchell, P. and Tjian, R. (1987). Purified transcription factor AP-1 interacts with TPA-inducible enhancer elements. *Cell* **49**, 741-752.
Mechta-Grigoriou, F., Gerald, D. and Yaniv, M. (2001). The mammalian Jun proteins: redundancy and specificity. *Oncogene* **20**, 2378-2389.
Newman, A. P., White, J. G. and Sternberg, P. W. (1995). The Caenorhabditis elegans lin-12 gene mediates induction of ventral uterine specialization by the anchor cell. *Development* **121**, 263-271.
Newman, A. P., White, J. G. and Sternberg, P. W. (1996). Morphogenesis of the C. elegans hermaphrodite uterus. *Development* **122**, 3617-3626.
Newman, A. P., Acton, G. Z., Hartwieg, E., Horvitz, H. R. and Sternberg, P. W. (1999). The *lin-11* LIM domain transcription factor is necessary for morphogenesis of C. elegans uterine cells. *Development* **126**, 5319-5326.
Newman, A. P., Inoue, T., Wang, M. and Sternberg, P. W. (2000). The Caenorhabditis elegans heterochronic gene lin-29 coordinates the vulval-uterine-epidermal connections. *Curr. Biol.* **10**, 1479-1488.
O'Shea, E. K., Rutkowski, R. and Kim, P. S. (1992). Mechanism of specificity in the Fos-Jun oncoprotein heterodimer. *Cell* **68**, 699-708.
Radtke, F., Wilson, A. and MacDonald, H. R. (2004). Notch signaling in T- and B-cell development. *Curr. Opin. Immunol.* **16**, 174-179.
Ramirez-Carrozzi, V. and Kerppola, T. (2003). Asymmetric recognition of nonconsensus AP-1 sites by Fos-Jun and Jun-Jun influences transcriptional cooperativity with NFAT1. *Mol. Cell. Biol.* **23**, 1737-1749.
Rebeiz, M., Reeves, N. L. and Posakony, J. W. (2002). SCORE: a computational approach to the identification of cis-regulatory modules and target genes in whole-genome sequence data. Site clustering over random expectation. *Proc. Natl. Acad. Sci. USA* **99**, 9888-9893.
Rimann, I. and Hajnal, A. (2007). Regulation of anchor cell invasion and uterine cell fates by the egl-43 Evi-1 proto-oncogene in Caenorhabditis elegans. *Dev. Biol.* **308**, 187-195.
Seydoux, G. and Greenwald, I. (1989). Cell autonomy of lin-12 function in a cell fate decision in C. elegans. *Cell* **57**, 1237-1245.
Seydoux, G., Savage, C. and Greenwald, I. (1993). Isolation and characterization of mutations causing abnormal eversion of the vulva in Caenorhabditis elegans. *Dev. Biol.* **157**, 423-436.
Sherwood, D. R. and Sternberg, P. W. (2003). Anchor cell invasion into the vulval epithelium in C. elegans. *Dev. Cell* **5**, 21-31.
Sherwood, D. R., Butler, J. A., Kramer, J. M. and Sternberg, P. W. (2005). FOS-1 promotes basement-membrane removal during anchor-cell invasion in C. elegans. *Cell* **121**, 951-962.
Sternberg, P. W. (1988). Lateral inhibition during vulval induction in Caenorhabditis elegans. *Nature* **335**, 551-554.
Sternberg, P. W. and Horvitz, H. R. (1989). The combined action of two intercellular signaling pathways specifies three cell fates during vulval induction in C. elegans. *Cell* **58**, 679-693.
Tamura, K., Taniguchi, Y., Minoguchi, S., Sakai, T., Tun, T., Furukawa, T. and Honjo, T. (1995). Physical interaction between a novel domain of the receptor Notch and the transcription factor RBP-J kappa/Su(H). *Curr. Biol.* **5**, 1416-1423.
Trent, C., Tsuing, N. and Horvitz, H. R. (1983). Egg-laying defective mutants of the nematode Caenorhabditis elegans. *Genetics* **104**, 619-647.
Tulchinsky, E. (2000). Fos family members: regulation, structure and role in oncogenic transformation. *Histol. Histopathol.* **15**, 921-928.
Vogt, P. K. (2001). Jun, the oncoprotein. *Oncogene* **20**, 2365-2377.
Weng, A. P. and Aster, J. C. (2004). Multiple niches for Notch in cancer: context is everything. *Curr. Opin. Genet. Dev.* **14**, 48-54.
Wilkinson, H. A., Fitzgerald, K. and Greenwald, I. (1994). Reciprocal changes in expression of the receptor lin-12 and its ligand lag-2 prior to commitment in a C. elegans cell fate decision. *Cell* **79**, 1187-1198.
Yoo, A. S., Bais, C. and Greenwald, I. (2004). Crosstalk between the EGFR and LIN-12/Notch pathways in C. elegans vulval development. *Science* **303**, 663-666.
Yu, H., Yoo, A. S. and Greenwald, I. (2004). Cluster analyzer for transcription sites (CATS): a C++-based program for identifying clustered transcription factor binding sites. *Bioinformatics* **20**, 1198-1200.